

danger associated with assigning linear segments to ionization efficiency curves is once again emphasized. More detailed results for oxygen will soon be submitted for publication along with results for nitrogen, hydrogen, and the rare gases.

†Work supported in part by Project DEFENDER of the Advanced Research Projects Agency, Department of Defense, under Office of Naval Research Contract No. Nonr-2786(00), and in part by the Defense Atomic Support Agency under Contract No. DA49-146-XZ-041.

*Present address: St. Francis University, Antigonish, Nova Scotia.

‡Present address: University of Texas, Austin, Texas. Robert A. Welch Foundation Grantee.

¹Ionization in H₂: P. Marmet and L. Kerwin, *Can. J. Phys.* **38**, 972 (1960); L. Kerwin, P. Marmet, and E. M. Clarke, *Can. J. Phys.* **31**, 1240 (1960). Ionization in N₂: P. Marmet and J. D. Morrison, *J. Chem. Phys.* **36**, 1238 (1962).

²C. E. Brion, *J. Chem. Phys.* **40**, 2995 (1964).

³C. E. Melton and W. H. Hamill, *J. Chem. Phys.* **41**, 546 (1964); and references pertinent to ionization of O₂.

⁴A. J. C. Nicholson, *J. Chem. Phys.* **39**, 954 (1963); and references pertinent to photoionization of O₂.

⁵G. H. Wannier, *Phys. Rev.* **100**, 1180 (1956); S. Geltman, *Phys. Rev.* **102**, 171 (1956); and an excellent extension of this work by F. H. Dorman, J. D. Morrison, and A. J. C. Nicholson, *J. Chem. Phys.* **32**, 378 (1960).

⁶J. D. Morrison, *J. Chem. Phys.* **40**, 2488 (1964).

⁷W. L. Fite and R. T. Brackmann, *Phys. Rev.* **112**, 1141 (1958).

⁸S. N. Foner and R. L. Hudson, *J. Chem. Phys.* **36**, 2681 (1962).

⁹At the moment we can suggest but one possible explanation for this discrepancy. Indirect heating of the gas by the filament might have a much larger effect on the ionization efficiency curve than previously suspected. In our experiments we are presently using a chopped room-temperature beam which passes unimpeded through the collision region. Preliminary experiments in which we preheat the beam give ionization efficiency curves which somewhat resemble those previously published. (See references 1 and 2 above.)

¹⁰G. Herzberg, *Spectra of Diatomic Molecules* (D. Van Nostrand Company, Inc., New York, 1950).

¹¹M. E. Wacks and M. Krauss, *J. Chem. Phys.* **35**, 1902 (1961).

SCATTERING CROSS SECTION OF IDEAL GASES FOR NARROW LASER BEAMS

O. Theimer*

University of California, Los Alamos Scientific Laboratory, Los Alamos, New Mexico

(Received 8 October 1964)

Recent experiments by George *et al.*¹ have indicated that Rayleigh's theory may not be valid for scattering of narrow laser beams by ideal gases. It will be shown in this Letter that interference phenomena do, in fact, produce deviations from Rayleigh's theory which are significant if the scattering volume satisfies certain criteria of smallness, and that these interference effects can explain some of the above-mentioned striking experimental results.

For a derivation of the modified scattering formula, consider a system of N molecules with polarizability α in a large cubical volume $V = L^3$. The scattering volume v is that section of the incident laser beam which is seen by the detector and is assumed much smaller than V . In many practical cases v is approximately a parallelepiped, as shown in Fig. 1. Its volume is

$$v = abc/\sin\theta, \quad (1)$$

where θ is the scattering angle, and a , b , c are, respectively, the width and height (along z) of the laser beam, and the width of the scattered beam (determined by diaphragms). According to Eq. (1), the scattering volume and with it the intensity are proportional to $1/\sin\theta$. This is characteristic for scattering of narrow beams,² but it appears that this trivial angle dependence has been neglected by George *et al.*

An incident monochromatic radiation field with frequency ω and space dependence

$$\vec{E}(\vec{r}) = \vec{E} \exp(i\vec{k}\cdot\vec{r}), \quad k = 2\pi/\lambda, \quad (2)$$

induces a dipole moment

$$\vec{p}(\vec{r}_j) = \alpha \vec{E}(\vec{r}_j) = \vec{p} \exp(i\vec{k}\cdot\vec{r}_j) \quad (3)$$

in the molecule located at \vec{r}_j . \vec{p} , oscillating with the frequency ω , is the source of a scattered radiation field³

$$\vec{E}_j'(\vec{D}) = f(\vec{R}, \lambda, \theta) \exp[i(\vec{k}\cdot\vec{r}_j + kR)], \quad (4)$$

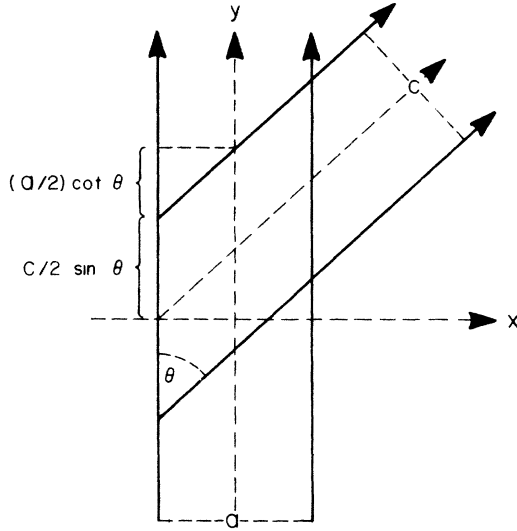


FIG. 1. Scattering geometry. Incident beam (width a) along y . Scattered beam (width c) makes angle θ with y .

where \vec{D} is the position of a distant detector, $\vec{R} = \vec{D} - \vec{r}_j$, and

$$\vec{f}(\vec{R}, \lambda, \theta) = -(4\pi^2/R^3\lambda^2)[\vec{R} \times (\vec{R} \times \alpha \vec{E})]. \quad (5)$$

If $D \gg \vec{r}_j$ for all molecules in v ,

$$R = D - (\vec{r}_j \cdot \vec{D})/D, \quad (6)$$

and writing

$$k\vec{D}/D = \vec{k}', \quad \vec{k} - \vec{k}' = \vec{\mu}, \quad \vec{f}(\vec{R}, \lambda, \theta) \approx \vec{f}(\vec{D}, \lambda, \theta), \quad (7)$$

the total radiation field scattered by the volume v is

$$\begin{aligned} \vec{E}'(\vec{D}) &= \sum_{j \text{ in } v} \vec{E}_j'(\vec{D}) \\ &= \vec{f}(\vec{D}, \lambda, \theta) \exp(ikD) \sum_{j \text{ in } v} \exp(i\vec{\mu} \cdot \vec{r}_j). \end{aligned} \quad (8)$$

The sum over j may be transformed into an integral over v by means of the fine-grained particle density

$$n(\vec{r}) = \sum_{j=1}^N \delta(\vec{r} - \vec{r}_j) = \sum_{\vec{q}} n_{\vec{q}} \exp(i\vec{q} \cdot \vec{r}), \quad (9)$$

$$\begin{aligned} n_{\vec{q}} &= n_{-\vec{q}}^* = \frac{1}{V} \sum_{j=1}^N \exp(-i\vec{q} \cdot \vec{r}_j) \text{ if } \vec{q} \neq 0, \\ &= n_0 \text{ if } \vec{q} = 0, \end{aligned} \quad (10)$$

$$q_i = 2\pi h_i/L, \quad h_i = 0, \pm 1, \pm 2, \pm \dots, \quad i = x, y, z. \quad (11)$$

Eq. (8) may now be written in the form

$$\begin{aligned} \vec{E}'(\vec{D}) \\ = \vec{f}(\vec{D}, \lambda, \theta) \exp(ikD) \sum_{\vec{q}} n_{\vec{q}} \int_v \exp[i\vec{r} \cdot (\vec{\mu} + \vec{q})] d\vec{r}, \end{aligned} \quad (12)$$

and multiplying (12) with the complex conjugate $\vec{E}'^*(\vec{D})$ one obtains the differential scattering cross section per unit solid angle³ associated with a specific particle configuration,

$$\sigma(\theta, \lambda) = T(\theta, \lambda) |A_{\mu}|^2, \quad (13)$$

where

$$T(\theta, \lambda) = |\hat{e}' \cdot (\alpha \hat{e}) 4\pi^2/\lambda^2|^2 \quad (14)$$

is Thomson's scattering factor,⁴ \hat{e}' , \hat{e} are unit vectors in directions \vec{E}' and \vec{E} , and

$$\begin{aligned} A_{\mu} &= n_0 \int_v \exp(i\vec{r} \cdot \vec{\mu}) d\vec{r} \\ &+ \sum_{\vec{q} \neq 0} n_{\vec{q}} \int_v \exp[i\vec{r} \cdot (\vec{\mu} + \vec{q})] d\vec{r} \end{aligned} \quad (15)$$

is the scattering amplitude. The ensemble average $\langle \sigma(\theta, \lambda) \rangle$ taken over all particle configurations gives the time average of the scattering cross section integrated over the whole Doppler-broadened spectrum.

To evaluate the integrals in (15), let $(\vec{\mu} + \vec{q}) = \vec{Q}$ and note that the limits of y for a fixed value of x are $(x + \frac{1}{2}a) \cot \theta \pm c/2 \sin \theta$. Thus,

$$\begin{aligned} \int_v \exp(i\vec{r} \cdot \vec{Q}) d\vec{r} \\ = 8 \prod_{\nu} (\sin l_{\nu} U_{\nu} / U_{\nu}) \exp[\frac{1}{2}ia Q_y \cot \theta], \end{aligned} \quad (16)$$

with

$$l_1 = \frac{1}{2}a, \quad l_2 = c/2 \sin \theta, \quad l_3 = \frac{1}{2}b, \quad (17a)$$

$$U_1 = Q_x + Q_y \cot \theta, \quad U_2 = Q_y, \quad U_3 = Q_z. \quad (17b)$$

The quantity $\langle |A_{\mu}|^2 \rangle$ involves the ensemble averages of the products $\langle n_{\vec{q}} n_{\vec{q}'} \rangle$ which, for ideal gases, have the simple property⁵

$$\begin{aligned} \langle n_{\vec{q}} n_{\vec{q}'} \rangle &= \frac{1}{V^2} \langle \sum_j \sum_{j'} \exp[i(\vec{q} \cdot \vec{r}_j + \vec{q}' \cdot \vec{r}_{j'})] \rangle \\ &= \frac{1}{V^2} \langle \sum_j \sum_{j'} \exp[i\{(\vec{q} + \vec{q}') \cdot \vec{r}_j \\ &\quad + \vec{q}' \cdot (\vec{r}_{j'} - \vec{r}_j)\}] \rangle \end{aligned} \quad (18)$$

$$= n_0^2 \text{ if } q = q' = 0, \quad (18a)$$

$$= (n_0/V) \text{ if } \vec{q} + \vec{q}' = 0, \quad \vec{q}' \neq 0, \quad (18b)$$

$$= 0 \text{ otherwise.}$$

Hence, writing the contributions from (18a) and (18b) separately,

$$\begin{aligned} \langle |A_{\mu}^{-}|^2 \rangle &= 64 \sum_{\vec{q}} \sum_{\vec{q}'} \langle n_{\vec{q}} n_{\vec{q}'}^* \rangle \prod_{\nu} \frac{\sin l_{\nu} U_{\nu}}{U_{\nu}} \frac{\sin l_{\nu} U_{\nu}'}{U_{\nu}'} \\ &\quad \times \exp\left[\frac{1}{2} i a \cot \theta (Q_y - Q_y')\right], \\ &= 64 n_0^2 \prod_{\nu} \frac{\sin^2 l_{\nu} U_{\nu}}{U_{\nu}^2} \\ &\quad + \frac{64 n_0}{V} \sum_{\vec{q} \neq 0} \prod_{\nu} \frac{\sin^2 l_{\nu} U_{\nu}}{U_{\nu}^2}. \end{aligned} \quad (19)$$

Eq. (19) can be simplified on the basis of the following assumptions:

(i) According to the geometry of Fig. 1, the average value of μ_z is zero. However, because of the finite size of the scattering volume and the detector, μ_z is distributed over a small region in reciprocal space whose width along z is $\Delta\mu_z$. In most practical cases the product $l_z \Delta\mu_z \gg 1$ and the fraction γ of the scattered

radiation for which $|l_z \mu_z| \lesssim 1$ will be very small, say 1/1000, and a sensitive function of the experimental setup. By order of magnitude $\gamma \approx 2D/b\mu d$, where d is the diameter of the detector surface illuminated by the scattered radiation. Now, from (17)

$$\begin{aligned} \sin^2 l_z \mu_z / \mu_z^2 &= \frac{1}{4} b^2 \text{ if } l_z \mu_z \lesssim 1, \\ &\approx 1/\mu_z^2 \ll \frac{1}{4} b^2 \text{ if } l_z \mu_z > 1. \end{aligned} \quad (20)$$

Hence, the average of $\sin^2 l_z \mu_z / \mu_z^2$ over all μ_z is approximately

$$\langle \sin^2 l_z \mu_z / \mu_z^2 \rangle \approx \frac{1}{4} \gamma b^2. \quad (21)$$

(ii) The average values of μ_x and μ_y are quite different from zero with the exception of extreme forward scattering. The finite range $\Delta\mu_x$ and $\Delta\mu_y$ of these quantities allows the approximation

$$\langle \sin^2 l_{\nu} U_{\nu} / U_{\nu}^2 \rangle \approx \frac{1}{2} U_{\nu}^2, \quad \nu = 1, 2, \text{ if } l_{\nu} \Delta U_{\nu} > 1. \quad (22)$$

(iii) According to Eq. (11) the reciprocal vectors \vec{q} vary almost continuously if V is large. Thus, the sum in (19),

$$\sum_{\vec{q} \neq 0} \prod_{\nu} \frac{\sin^2 l_{\nu} U_{\nu}}{U_{\nu}^2} = \frac{V}{8\pi^3} \int \prod_{\nu} \frac{\sin^2 l_{\nu} U_{\nu}}{U_{\nu}^2} d\vec{q} = \frac{V}{8\pi^3} \prod_{\nu} \int \frac{\sin^2 l_{\nu} U_{\nu}}{U_{\nu}^2} dU_{\nu} = (V/8) \prod_{\nu} l_{\nu} = Vv/64. \quad (23)$$

In deriving (23) use has been made of Eqs. (1) and (17), and of the fact that the Jacobian of the transformation (18) is unity. Utilizing (21), (22), and (23),

$$\langle |A_{\mu}^{-}|^2 \rangle = A_R^2 + A_0^2 = n_0^2 v + (4b^2 \gamma / U_1^2 U_2^2) n_0^2. \quad (24)$$

The first term in Eq. (24) represents the number of molecules in the scattering volume and is identical with the scattering amplitude A_R^2 of Rayleigh's theory. In the present theory, A_R^2 is a contribution from the Fourier components of the particle density with $\vec{q} \neq 0$ and, hence, it represents scattering by density fluctuations. The term A_0^2 , which is produced by the average particle density n_0 , represents an interference effect which strongly increases when the width of the incident and scattered beam gets small.

According to Eqs. (19) and (1),

$$\lim_{v \rightarrow 0} A_0^2 = n_0^2 v^2. \quad (25)$$

Hence, whenever v is so small that $l_{\nu} \mu_{\nu} \ll 1$

for all ν and all scattering angles, then $A_0^2 \gg A_R^2$ and the scattering intensity is proportional to the square of the particle number in v . On the other hand, if Condition (ii) is satisfied, Eqs. (17), together with the geometry of Fig. 1, show that

$$A_0^2(\theta) = 4\gamma b^2 n_0^2 / [k^2 (1 - \cos \theta) \times (\cot \theta - \sin \theta - \cos \theta \cot \theta)]^2, \quad (26)$$

$$A_0^2(60) = 48\gamma b^2 n_0^2 / k^4 = 12A_0^2(90), \quad (27)$$

$$\begin{aligned} \epsilon(60) &= A_0^2(60) / A_R^2(60) = 3\sqrt{3} \gamma n_0 \lambda^4 / 2\pi^4 c \\ &= 6\sqrt{3} \epsilon(90), \text{ if } a = b. \end{aligned} \quad (28)$$

These formulas are in fair agreement with the experimental results presented in Fig. 3 of reference 1 if $\epsilon(90) \approx 0.004$, i.e., $c/\gamma \approx 300$ (see Fig. 2). They do not explain the striking effect of the polarization of the incident beam reported in reference 1 since this polarization affects only the Thomson factor $T(\theta, \lambda)$ in the present theory. But there is a possibility that

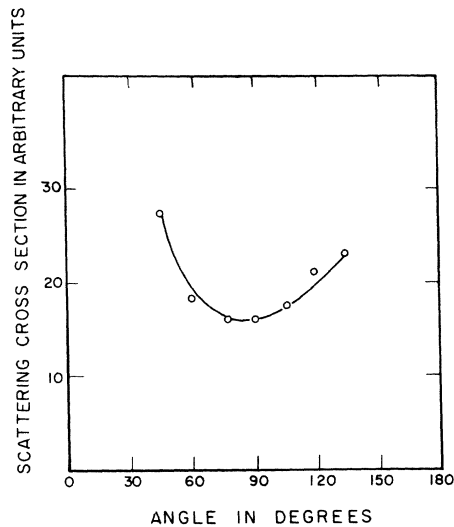


FIG. 2. Total scattering cross section of argon at normal pressure and temperature ($n_0 = 2 \times 10^{19} \text{ cm}^{-3}$) for ruby-laser ($\lambda = 6934 \text{ \AA}$) beam polarized normal to scattering plane. Full line calculated from Eqs. (24) and (26); circles are experimental points reported by George *et al.*¹

γ depends on the polarization if the laser beam is not symmetric about its axis. Finally, if $\epsilon(60)$ were approximately unity, as is implied in Table I of reference 1, the forward bias of the scattering predicted by Eq. (26) would be much larger than that observed by experiment. It is obvious that more accurate experiments and a theory which takes into account the exact shape of the scattering volume, the intensity

distribution in the incident beam, and the solid angle of the scattered beam, are required for explaining the apparent discrepancies between theory and experiment. Such a detailed analysis may profit from the fact that n_0 is constant in space and time for gases which are in thermal equilibrium and free of turbulence. Consequently, scattering associated with the term A_0^2 has exactly the frequency ω of the incident radiation field. On the basis of this property, it can be experimentally distinguished from scattering associated with density fluctuations which is always Doppler shifted in ideal gases.

*On leave from New Mexico State University, Research Center, University Park, New Mexico.

¹T. V. George, L. Slama, M. Yokoyama, and L. Goldstein, *Phys. Rev. Letters* **11**, 403 (1963).

²Formula (1) breaks down for small scattering angles since the effective length, $c/\sin\theta$, of the scattering volume is always smaller than an upper limit determined by diaphragms, or the walls of the gas container.

³W. K. Panofsky and M. Phillips, *Classical Electricity and Magnetism* (Addison-Wesley Publishing Company, Inc., Reading, Massachusetts, 1956), 2nd ed., p. 322 ff.

⁴Usually the Thomson factor is given for natural incident light and free electrons with polarizability $e^2\lambda^2/4\pi^2c_0^2m_e$ (c_0 = vacuum velocity of light, m_e = electron mass). In this case $T(\theta, \lambda) = (e^4/c^4m^2) \times (1 + \cos^2\theta)/2$.

⁵In plasmas, $\langle n_0 n_1 \rangle$ depends on the radial distribution function of electrons about electrons.

FINAL-STATE INTERACTIONS IN THE REACTION $\text{He}^3(d, t)2p$ AT 24.7 AND 33.4 MeV

H. E. Conzett, E. Shield, R. J. Slobodrian, and S. Yamabe*

Lawrence Radiation Laboratory, University of California, Berkeley, California

(Received 3 November 1964)

Recent Letters have reported experimental determinations of triton energy spectra from the reaction $\text{He}^3(d, t)$ at $E_d = 28 \text{ MeV}$ ¹ and at 20 and 25 MeV.² The spectra of reference 1 were obtained with approximately 1.25-MeV energy resolution, and a broad peak near the high-energy end was interpreted as resulting from the formation of an unbound state of He^2 with a mean lifetime $\tau = (0.2 \pm 0.1) \times 10^{-21} \text{ sec}$. The observed angular variation of the peak was consistent with a pick-up reaction mechanism. The spectra of reference 2 were ob-

tained with an energy resolution of about 0.5 MeV and consisted of continuum spectra with broad asymmetrical peaking near the high-energy limit. These authors noted a resemblance to neutron spectra from the reaction^{3,4} $D(p, n)2p$, whose shape was explained in terms of a final-state interaction^{5,6} between the two protons and they pointed out the necessity both for more precise data and for quantitative calculations in the continued investigation of this reaction [$\text{He}^3(d, t)2p$].

We report here experimental results along